J. Fluid Mech. (1995), vol. 298, pp. 139–165

The structure and control of a turbulent reattaching flow

By L. W. SIGURDSON

Department of Mechanical Engineering, University of Alberta, Edmonton, Alberta, Canada, T6G 2G8

(Received 8 December 1993 and in revised form 17 December 1994)

An experimental study was made of the effect of a periodic velocity perturbation on the separation bubble downstream of the sharp-edged blunt face of a circular cylinder aligned coaxially with the free stream. Velocity fluctuations were produced with an acoustic driver located within the cylinder and a small circumferential gap located immediately downstream of the fixed separation line to allow communication with the external flow. The flow could be considerably modified when forced at frequencies lower than the initial Kelvin–Helmholtz frequencies of the free shear layer, and with associated vortex wavelengths comparable to the bubble height. Reattachment length, bubble height, pressure at separation, and average pressure on the face were all reduced. The effects on the large-scale structures were studied using flow photographs obtained by the smoke-wire technique. The forcing increased the entrainment near the leading edge. It was concluded that the final vortex of the shear layer before reattachment is an important element of the flow structure. There are two different instabilities involved: the Kelvin–Helmholtz instability of the free shear layer and the 'shedding'-type instability of the entire bubble. The former consists of an interaction of the shear layer vorticity with itself, the latter with its images that result because of the presence of a wall. In order to determine the optimum forcing frequency, a method of frequency scaling is proposed which correlates data for a variety of bubbles and supports an analogy with Kármán vortex shedding.

1. Introduction

Investigators of free shear layers have discovered that organized large-scale vortical structures play an important role in the dynamics of the flow (Brown & Roshko 1974; Winant & Browand 1974). It was also found that periodic forcing of these structures can modify their development and consequently the growth of the shear layer (Oster & Wygnanski 1982; Roberts 1985). The purpose of the present investigation is to study the effect of a periodic velocity perturbation on a separation bubble, where the separated shear flow begins its development as a free shear layer but undergoes interaction with the wall at reattachment and ultimately becomes a boundary layer flow farther downstream. A study was made of the effect of a periodic velocity perturbation on the separation bubble downstream of the sharp-edged blunt face of a circular cylinder aligned coaxially with the free stream. It was part of a larger research effort to characterize the structure of reattaching flows in general. Reattaching flows are common in several engineering devices, such as external flows over semi-trailers, aircraft wings, compressor blades, and internal flows such as diffusers and backward-facing steps. An understanding of the potential to control the flow for improved performance is very important. The coaxial cylinder was chosen here as a simple test

case. An excellent review of the literature concerning the general case of separation control and its benefits is given by Gad-el-Hak & Bushnell (1991).

Some of the earliest published work to use unsteady forcing on reattaching flows was done on the flow over wings and rearward-facing ramps and steps. Collins & Zelenevitz (1975) concluded that 'external sound can cause partial reattachment of the flow about a stalled airfoil, greatly increasing the lift and decreasing the pressure drag'. Viets (1979) showed that a cam-shaped rotor inset into the wall immediately upstream of a ramp diffuser could affect the pressure distribution on the ramp and the ability of the flow to remain attached. Viets & Platt (1981) showed that a similar device for a backward-facing step (a dump combustor type of geometry) could create a more rapid and substantial pressure rise with downstream distance and reduce the reattachment length (the distance from separation to reattachment). It was found that the effect of rotor speed and therefore frequency of vortex generation was important for positive effects on performance. The rotor was found to enhance the interaction between the flame holding recirculation region and the main flow. The conditions for optimum frequency of rotation were not well understood.

With this as a background, the current study was undertaken to learn the possible positive effects of forcing on the coaxial cylinder separation bubble. The bubble length, pressure at separation, and forebody drag (defined as the average pressure on the cylinder face) were investigated. The effects on the bubble structure, and especially on the turbulent structures of the free shear layer, were studied using flow photographs and films obtained with the smoke-wire technique in a wind tunnel. The shear layer appeared to be laminar at separation in all photographs. The laser-induced-fluorescence technique was used in water for the unforced case. Early results were reported by Sigurdson, Cimbala & Roshko (1981). They found that when forcing at some frequencies close to or lower than the initial Kelvin–Helmholtz instability of the shear layer, reattachment occurred sooner, and the pressure at separation (and therefore the drag on the cylinder face) was lowered. The maximum reduction in drag was possible when the forcing frequency was such that the associated vortex size was comparable to the separated region's thickness; no pairing of the vortices occurred and the vortices convected along the surface of the cylinder. The primary questions that resulted were how the forcing caused these results and how to determine the frequency of excitation for the maximum effect.

In order to answer both these questions, something must be known about the mechanisms of the natural unforced bubble vortex structure. After a review of other research and apparatus, in the following sections the experimental results will be presented and discussed in this light, §§3, 4.1. It will be shown how this led to a hypothesis that not only the Kelvin–Helmholtz instability was at work, but also another instability much like the Kármán vortex shedding instability in the wake of a transverse cylinder, §4.2. This hypothesis offers a categorization for different regimes of forcing frequency for the bubble, §4.3, and the necessity to determine how the frequencies scale, §§4.4, 4.5. The hypothesis is tested by applying the proposed scaling to the results for the unforced and forced bubbles, §§4.6, 4.7, as well as to the results from other geometries, §4.8, where an apparent universality is shown to hold.

The majority of the ideas were previously reported by Sigurdson & Roshko (1985, 1988) and, with additional supporting data, by Sigurdson (1986). The present work is essentially a revision of part of the latter thesis, with updated reference to and comparison with research that has been published since.

Other work on the unforced coaxial cylinder separation bubble has been done by Ota (1975) and Ota & Motegi (1980) who measured the pressures, velocities and

geometry of the bubble, but made no comment on the large-scale structures rear reattachment. Kiya *et al.* (1991*a*) measured several of the turbulence properties including the frequency of the large-scale structures at reattachment. They referred to the importance of information on the large-scale vortices in the reattachment region and how Sigurdson (1986) and Sigurdson & Roshko (1988) demonstrated that they can be controlled. Kiya *et al.* (1991*b*) and Shimizu *et al.* (1993) used an apparatus which seems to be patterned after (it is almost identical to) that described here and in Sigurdson & Roshko (1985). They conducted forced experiments in air, with similar results which will be described and compared later, §4.7. Kiya *et al.* (1991*b*) agreed with Sigurdson & Roshko (1985) that the reattachment length could be reduced for select single forcing frequencies, but also experimented with bimodel forcing frequencies which they found were more effective than the single frequency. Shimizu *et al.* (1993) found that the curve of the reattachment length versus single frequency excitation attained a single minimum for low and high forcing levels, but two minima for intermediate forcing levels. They also found that the reattachment length could be slightly increased when forcing at frequencies approximately one-half of the free shear layer Kelvin–Helmholtz instability frequency near separation. Kiya *et al.* (1993*a*, *b*) report careful measurements of the velocities in the bubble with a laser Doppler velocimeter for the same type of apparatus but in water rather than air, with a consequently narrower range of forcing frequency, and lower Reynolds numbers. None of the above work offers an explanation of how the optimum frequency is selected. This paper contributes to that question.

The two-dimensional analogue of the coaxial cylinder, the square-edged flat plate, has been the subject of several investigations. It was for this flow that the idea of the reattachment zone being dominated by large-scale vortex structures appeared. Lane & Loehrke (1980) noted 'two-dimensional rolls' while studying the transition of the bubble. Hillier & Cherry (1981) found large vortical structures while studying the effect of free-stream turbulence on the bubble and noted that it caused a reduction in reattachment length. Similar results were found by Kiya & Sasaki (1983*a*). Kiya, Sasaki & Arie (1982) observed them in a discrete-vortex numerical simulation. Kiya & Sasaki (1983*b*) gave an excellent review of these observations and measured several features of the vortices, including the frequency which they are shed downstream of the bubble. Cherry, Hillier & Latour (1983, 1984) also contributed extensively to measurements of the unsteady aspects of the structures. They suggested that the bubble length could be used to non-dimensionalize various geometries. The three-dimensional nature of the structures is discussed by Sigurdson & Roshko (1984), Kiya & Sasaki (1985), Sigurdson (1986) and Sasaki & Kiya (1991). There have been forcing experiments on the flat-plate Kármán vortex shedding by Welsh & Gibson (1979) and Parker & Welsh (1983), and on the separation bubble by Soria, Sheridan & Wu (1993). Parker & Welsh concluded that, in general, the reattachment length was reduced when sound was applied. The present paper will discuss some of these flat-plate results with respect to the frequency of the vortical structures and how it can be universally scaled.

Research has been done on the effects of various types of forcing on other flow geometries (grouped by area in roughly chronological order of development): flows over wings (Collins & Zelenevitz 1974; Collins 1981; Ahuja, Whipkey & Jones 1983; Zaman, Bar-Sever & Mangalam 1987; Huang, Maestrello & Bryant 1987; Bar-Sever 1989; Gad-el-Hak 1990; Hsiao, Liu & Shyu 1990; Zaman 1992), a sharp-edged circular pipe inlet (Sutton *et al.* 1981), the flow behind an oscillating spoiler-like flap in a turbulent boundary layer with and without upstream separation (Koga, Reisenthel & Nagib 1984; Montividas, Acharya & Metwally 1992), backward-facing steps

(Bhattacharjee, Scheelke & Troutt 1986; Roos & Kegelman 1986; Miau *et al.* 1991) and an oscillating bluff plate mounted perpendicularly to a wall (Kelso, Lim & Perry 1993). Many of these efforts refer to previous reporting of the present work. Observations have been made of increased entrainment, reduced reattachment length, and what frequencies bring about optimum results. Although the coaxial cylinder geometry is different from the geometries investigated, useful application of the ideas presented here to correlate the frequencies in these flows will be discussed in §4.8.

In summary, it is now generally known that the reattachment region of a separation bubble is dominated by large-scale vortical structures and much headway has been made in describing them and attempting to force them. However, the mechanism by which the instability sustains itself and how forcing interacts with it optimally remain unclear. The present paper will contribute to these issues.

2. Experimental apparatus

The experiment was conducted in an open-return low-turbulence wind tunnel with flow velocity variable from 0.5 to 12 m s^{-1}. The r.m.s. turbulence intensity of the free stream was measured to be 0.4% at $U_\infty = 2$ m s^{-1}. The test section was 2 m long and 0.51 m square, resulting in a model blockage of 8.3% based on the cylinder cross-sectional area. No attempt has been made to correct the measurements for blockage. The measured effects of forcing are therefore specific to this particular geometry. Some photographs were obtained in the low-speed water channel also located in the Graduate Aeronautical Laboratories of the California Institute of Technology.

Figure 1 is a schematic of the flow mean streamlines and a cross-sectional view of the flat-faced cylinder. The forcing technique is to produce acoustic waves inside the cylinder by oscillation of the speaker located there. These are communicated to the flow through a small circumferential gap located just downstream of the separation line. This allows velocity fluctuations to be superimposed on the external flow.

The main cylinder was 16.5 cm in diameter (D) with 0.64 cm thick walls and was constructed out of Plexiglas. The front face was of 1.27 cm thick Plexiglas connected to the main body of the cylinder by three 0.32 cm diameter bolts. A 0.64 cm gap was left between the face plate and the main body of the cylinder.

A 12.7 cm woofer acoustic speaker was mounted within the cylinder. It was driven by a 50 W MacIntosh power amplifier with a sinusoidal output of controllable frequency and amplitude. The amplifier was driven by a Wavetek Model 148 signal generator. The voltage amplitude to the woofer had to be carefully controlled owing to a number of resonant frequencies in the forcing system. A calibration was performed to keep the velocity perturbation measured at the gap constant over a range of frequencies. The r.m.s. amplitude of the velocity perturbation (u') through the gap was measured using a hot wire with the wind tunnel flow off. A biasing flow over the hot wire was provided to avoid the rectification problems associated with flows having zero average velocity. In this way the necessary voltage to drive the woofer could be determined for each frequency. It was found that at a fixed frequency the velocity perturbation was linear with voltage. The hot wire was also used to select frequencies at which harmonics were minimal.

When comparing the results of this experiment to other forcing experiments where the velocity perturbation amplitude is controlled, the following should be kept in mind. The u' measurement in this experiment was taken in the middle of the gap behind the leading edge. If there were no reflections from the tunnel walls, the amplitude of perturbation would be expected to decrease with radial distance (r) from the gap

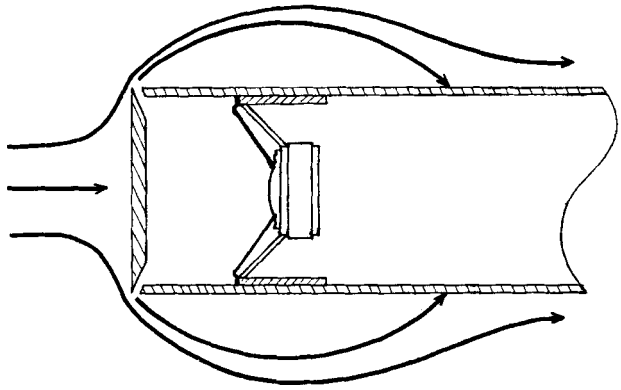

FIGURE 1. Cross-sectional view of the cylinder.

slightly faster than $1/r$, which would occur for a two-dimensional source. Consequently, the forcing amplitude in this case dropped off very rapidly away from the separation line, as opposed to experiments with free shear layers where the entire free stream is perturbed. This makes it difficult to compare the amplitudes presented here with other forced free shear layer experiments, some of which (Roberts 1985) have an approximately uniform velocity perturbation.

The mean pressure in the cavity ahead of the speaker was measured with a Barocel electronic manometer and was used to calculate the pressure coefficient (C_{p_s}) at the separation line. The dynamic pressure was measured upstream of the model with a Pitot static tube. The time-averaged reattachment location (X_r) was measured by visual inspection of tufts attached to the model. It was judged to occur where the oscillating tufts spent equal time pointing upstream and downstream. This allowed accuracy to better than 0.1 diameters.

Flow visualization was performed with a smoke-wire illuminated by a General Radio stroboscope. The electronic synchronizing controller for their operation was built at the Illinois Institute of Technology where the technique was developed. For further details see Corke *et al.* (1977).

3. Experimental results

3.1. *Pressure, drag, and reattachment length*

C_{p_s} and X_r are both reduced with forcing. It is notable that they were never observed to increase under the effects of excitation. Figure 2 shows the distribution of negative C_p as a function of downstream distance from the leading edge (X) normalized with D. The non-dimensional frequency or Strouhal number ($St_D = F_{ex} D/U_\infty$) of excitation was 3.1. These data were measured on an earlier version of the experiment and are included here only to give a qualitative impression. It demonstrates that C_{p_s} becomes more negative and the length of the bubble is decreased with excitation. Tufts indicated that X_r/D decreased from 1.4 to 1.2.

Early results from the present experiment are given in figure 3. The Reynolds number was fixed at 132000 where ($Re_D = U_\infty D/\nu$). This corresponded to a free-stream velocity (U_∞) of 12 m s^{-1}. Two different r.m.s. amplitudes of excitation (u'/U_∞ as measured in the gap) were used: 3.9% and 7.8%. An estimate of the pressure drag coefficient on the cylinder face (C_{d_f}, which is the same as the average C_p on the face)

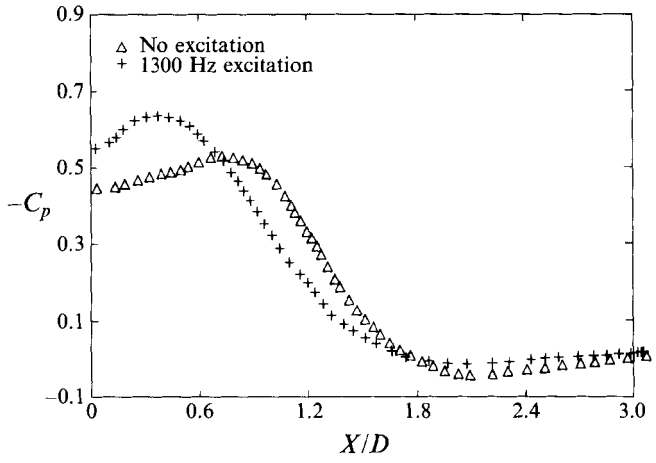

FIGURE 2. Pressure on the cylinder surface as a function of downstream distance.

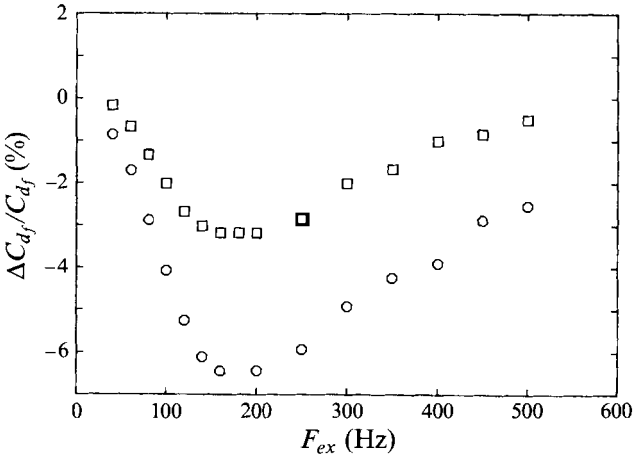

FIGURE 3. Percent change in pressure drag coefficient versus forcing frequency, $Re_D = 132000$ for two different r.m.s. amplitudes of excitation u'/U_∞: ○, 7.8%; □, 3.9%.

could be made from the measured C_{p_s} and empirical relations representing the drag on circular disks. This technique is discussed in Koenig (1978). The relation used here is

$$C_{d_f} = 0.8 + 0.2\, C_{p_s}. \tag{1}$$

The change in C_{d_f} normalized by the unforced value is plotted in figure 3 as a function of excitation frequency (F_{ex}).

There is a minimum in both curves for values of F_{ex} ranging between 150 and 200 Hz. This corresponds to values of $F_{ex} D/U_\infty$ ranging between 2 and 3, forming a 'drag bucket'. The magnitude of the minimum scales with the excitation amplitude: a 3.2% drag reduction for 3.9% forcing amplitude, and a 6.4% reduction for 7.8% forcing. The corresponding effect on C_{p_s} was stronger: a reduction of 10% and 17% for the two cases respectively. For larger forcing amplitudes, there was evidence that the effect saturates and the drag reduction tapers off.

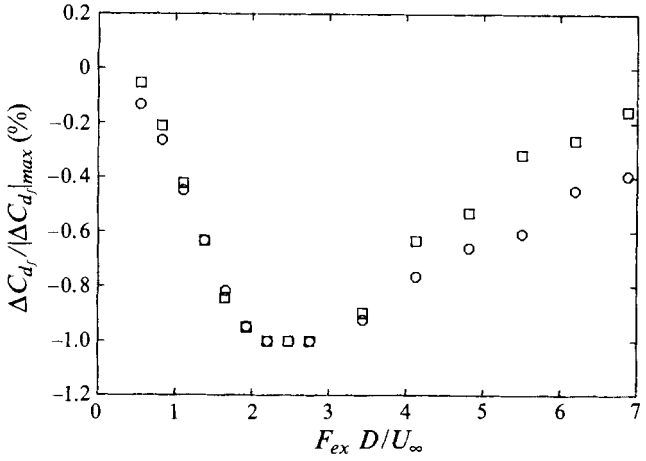

FIGURE 4. Normalized percent change in pressure drag versus forcing frequency, $Re_D = 132000$. Symbols as figure 3.

The same data are replotted in figure 4, but normalized with the maximum drag reduction and plotted versus $F_{ex}D/U_\infty$. It is interesting that the curves collapse very well for $F_{ex}D/U_\infty$ less than that for minimum drag, but diverge for the $F_{ex}D/U_\infty$ greater than that for the minimum. This suggests that the flow responds linearly to the lower frequencies, but nonlinearly to the higher ones. This will be discussed in §4.7.

The results were very sensitive to the presence of harmonics in the excitation. With all the other flow parameters held constant, the drag reduction was usually greater with harmonics present. Figures 3 and 4 contain measurements at frequencies preselected for their pureness of tone. X_r/D was reduced by a maximum of 30% and 20% for the 7.8% and 3.9% forcing amplitudes respectively. It behaved monotonically with C_{d_f}; as the drag was lowered the bubble became shorter. The reattachment length for the unforced case was $X_r/D = 1.2$. This is less than the value of 1.6 found by Ota (1975) for a cylinder in a flow with less blockage. The higher blockage in the present case accounts for both the shorter bubble length and the lower value of $C_{p_s} = -1.05$ for the unexcited case, as compared to -0.6 from Ota (1975).

3.2. *Flow visualization results*

A series of smoke-wire photographs (figure 5) were taken at $F_{ex}D/U_\infty = 0$ (no excitation), 20, 12, 8 and 4, with all other parameters fixed: ($U_\infty = 4$ m s^{-1}, $Re_D = 42400$, and $u'/U_\infty = 23\%$). The conditions were at a lower Re_D and higher u'/U_∞ than some of the C_{d_f} data presented here but will suffice to give a qualitative idea of the response of the flow to excitation. The smoke wire was located on the centreline 0.6 cm ahead of the cylinder face. If the smoke wire is placed farther ahead of the model, its wake becomes a problem as it encounters the stagnation region. Therefore, it must be located either very close to the model, so that the wake is weak due to the lower stagnation velocities, or very far, so that the wake has had time to diffuse.

The wavelength (λ_{ex}) of the vortices corresponding to the forcing should scale as follows:

$$\lambda_{ex} = U_c/F_{ex}, \tag{2}$$

where U_c is the convection velocity of the vortices. Figure 5 illustrates this result. For these values of $F_{ex}D/U_\infty$ and u'/U_∞, the frequency of the initial structures in the shear layer is identical to the forcing frequency. This conclusion was checked with a hot-wire

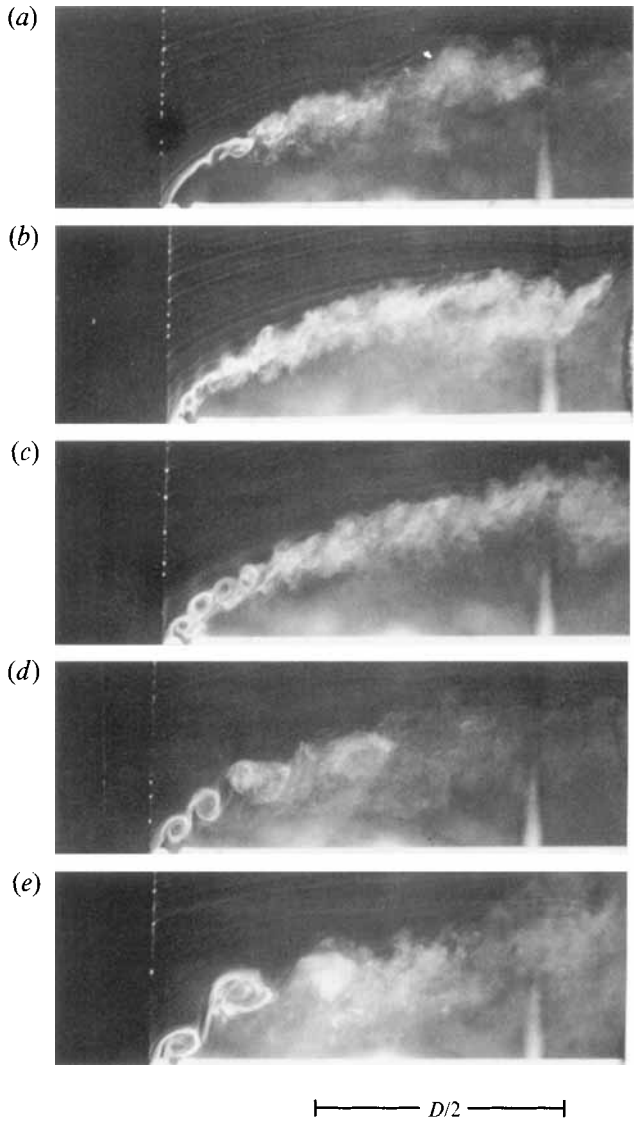

FIGURE 5. Smoke-wire visualization for $Re_D = 42400$, $u'/U_\infty = 23\%$ and varying forcing frequency: (*a*) $F_{ex}D/U_\infty = 0$, (*b*) 20, (*c*) 12, (*d*) 8, (*e*) 4.

anemometer. At this Re_D the initial Kelvin–Helmholtz instability of the shear layer has a frequency (F_{KH_i}) located in a broad band around 500 Hz, and a non-dimensional frequency of 20.6. The photos indicate that the initial structures lose their clarity within two or three wavelengths downstream of separation, which may be because of an amalgamation.

Figure 6(*a*) shows the flow with no excitation while figure 6(*b*) shows the flow with excitation at $F_{ex}D/U_\infty = 1.64$ and $u'/U_\infty = 12\%$. Both have $U_\infty = 2$ m s^{-1} and $Re_D = 22000$. The free streamlines calculated with a semi-empirical theory using the measured C_{p_b} are plotted over the photographs. They will be discussed in a following section.

The value of $F_{ex}D/U_\infty = 1.64$ is near the range of 2 to 3 where the minimum in C_{d_f} was measured (figure 4). The resulting vortex wavelength associated with this forcing

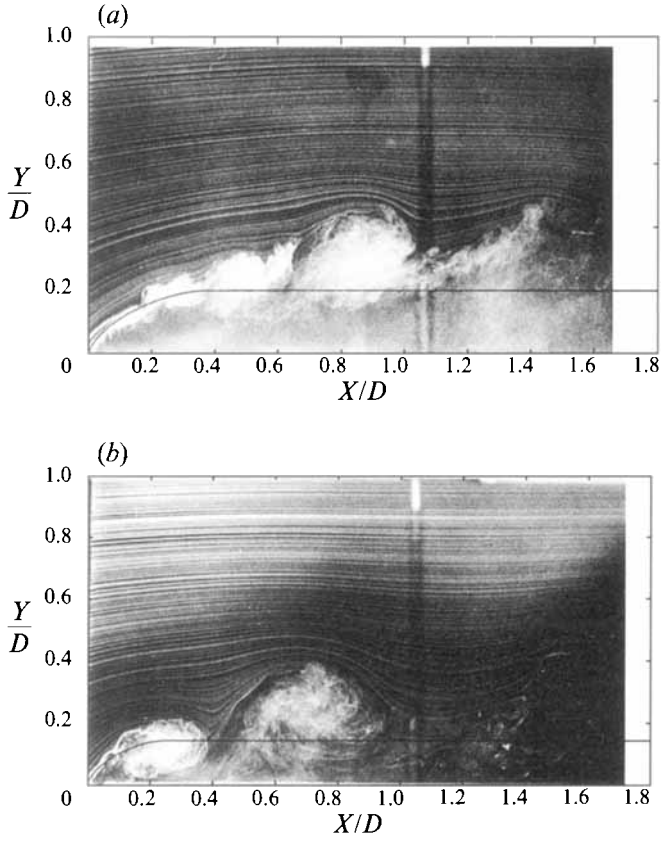

FIGURE 6. Smoke-wire flow visualization: (*a*) unforced; (*b*) forced, $F_{ex}D/U_\infty = 1.64$, $u'/U_\infty = 12\%$, $F_{ex}h/U_s = 0.16$. $Re = 22000$.

frequency is now so large that the vortex interacts with the wall almost immediately as it rolls up. Near separation, U_c can be approximated by $\frac{1}{2}U_s$, where

$$U_s/U_\infty = (1-C_{p_s})^{1/2} \tag{3}$$

is obtained using Bernoulli's equation (U_s is the velocity at the separation point). Substituting into (2) the result is

$$\frac{\lambda_{ex}}{D} = \frac{1}{2}\frac{U_s}{U_\infty}\left(\frac{F_{ex}D}{U_\infty}\right)^{-1}. \tag{4}$$

For the conditions in figure 6(*b*), λ_{ex}/D was calculated to be 0.46. This describes the structure located between $X/D = 0.4$ and 0.9 reasonably well. As that structure is just entering the reattachment region, U_c might be closer to one half the local free-stream velocity U'_∞ (greater than U_∞ owing to the tunnel blockage) rather than $\frac{1}{2}U_s$. The conclusion that $U_c = \frac{1}{2}U_\infty$ at reattachment was reported by Kiya & Sasaki (1983*b*). If an estimated U'_∞ of 1.16 U_∞ is substituted for U_s in (4), $\lambda_{ex}/D = 0.35$. A wavelength between these two values, 0.46 near separation and 0.35 closer to reattachment, would therefore be expected.

The large structure farthest downstream in the photograph has more than twice the wavelength of the initial structures corresponding to F_{ex}. It is surmised to result from

an amalgamation. Much smaller vortices can be seen near the separation line, with a wavelength associated with the initial Kelvin–Helmholtz instability. U_∞ was too low to use the tufts to measure X_r/D, but it would be 0.8 if X_r/D is assumed to scale linearly with the maximum height of the free streamline (h) plotted in figure 6(b).

4. Discussion

4.1. *How C_{d_f} is reduced*

The streaklines toward the top of the pictures in figure 6(a) and 6(b) indicate that the interference from the presence of the model is reduced in the excited case. They are much more curved and more inclined in the unexcited case. These observations are supported by measurements of the slope of the streaklines discussed later in this section. In the excited case it appears from the photographs that the large forced structures cause a large increase in entrainment close to the separation line. The increased entrainment (and correspondingly higher Reynolds stress) draws the irrotational flow closer to the model, resulting in time-averaged streamlines with a smaller radius of curvature near the separation line. The smaller radius maintains a higher radial pressure gradient, consequently C_{p_s} and therefore C_{d_f} are reduced (mainly because of the increased suction on the edge of the face). An alternative view is that as the streamlines are drawn nearer to the surface of the model, the external flow looks more like the potential flow solution around the body with no vorticity present, which has no separation, zero drag on the face, and a C_{p_s} reduced to negative infinity.

The reduced reattachment length is consistent with the increased growth rate of the shear layer. For backward-facing steps, Eaton & Johnston (1980, 1981) point out that X_r is determined by the growth rate of the shear layer and its curvature toward the wall. Sutton *et al.* (1981) state this for flow at a pipe inlet also. In the present case, both of these factors lead to a reduction in X_r. Figures 5 and 6 illustrate that the growth rate is increased, and the shear layer also does not have to grow as much before reaching the wall since the height of the bubble is decreased. The height of the bubble decreases owing to the increased entrainment that goes along with the increased growth rate. The increased entrainment from the low-speed side draws the shear layer closer to the wall, effectively decreasing bubble height. For blunt flat plates, Kiya & Sasaki (1983a) conjectured that a major role of free-stream turbulence in bringing about a reduced reattachment length is that it 'produces larger and larger vortices in a region a little downstream of the separation point'. Then 'larger vortices entrain fluid more efficiently than smaller vortices, thus yielding the shorter length of the separation bubble'. This is how the reattachment length is reduced in the present case.

In the present case, X_r was never found to increase under the influence of excitation, which might be expected when forcing at frequencies near F_{KH_i}. The vortices would be expected to 'lock-in' to the forcing frequency (Oster & Wygnanski 1982) which could inhibit growth of the shear layer as compared to the unforced case. By the reasoning given above, this would increase X_r. Shimizu *et al.* (1993) have observed a 4% increase in X_r (compared to the unforced case) when forcing at frequencies of approximately one half of F_{KH_i} and $u'/U_\infty = 4\%$. The present X_r measurement technique would not be able to detect this small change if it were present, and C_{p_s} was never observed to increase.

Attempts have been made to learn more about the effects of excitation on the entrainment by analysing the streakline photographs in figure 6. The slope of the streaklines (v/u where v is vertical velocity, u horizontal velocity, assuming steady flow) has been measured as a function of radial distance (R) from the axis of symmetry (figure

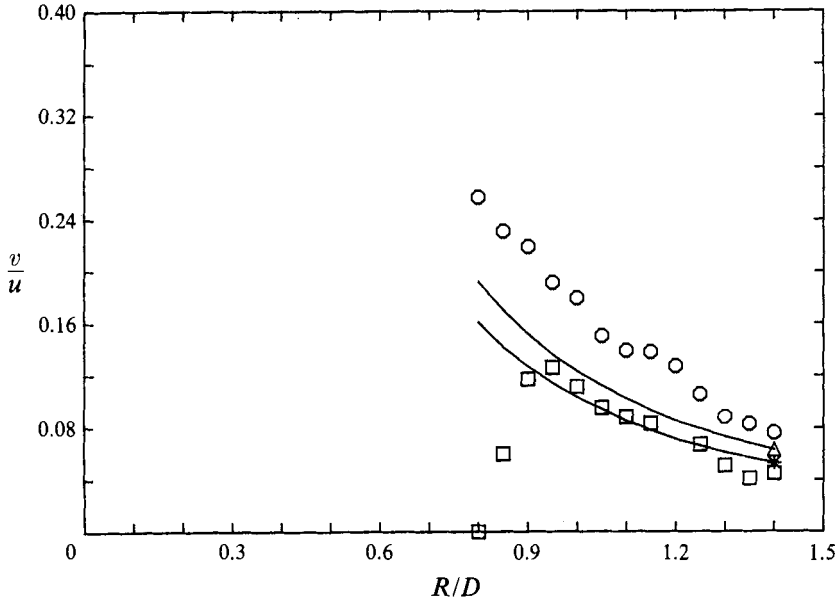

FIGURE 7. v/u versus radial distance. Experiment: ○, unforced; □, forced. Theory: △, unforced; ∗, forced.

7). This was compared to the results predicted from the exact solution for a Rankine body with a final diameter equal to that predicted by the free streamline theory. The slopes were measured at the same downstream distance from the cylinder face as the Rankine body source is from the front stagnation point, $X/D = 0.35$ and 0.33 respectively for figures 6(*a*) and 6(*b*). For large values of R the slopes decayed as $1/R^2$, as the theory predicted. The excited case also had values of v/u which were less than those for the unexcited case, consistent with the drag reduction in the excited case and an increased entrainment which reduces the value of v. The values of slope agreed with those for the Rankine body to within 30% for radial distances greater than one diameter for the unexcited case. With excitation, the agreement was excellent.

There are two primary reasons for disagreement. The strongest reason is that the theory does not account for the actual free streamline shape. The second is the flow unsteadiness in the photographs. Both of these effects are reduced with increased radial distance, and the agreement between theory and experiment is consequently improved. Similarly, agreement is better for the excited case since the body is smaller, therefore the distance from the surface of the body is relatively larger.

4.2. *Why $F_{ex}D/U_\infty$ has an optimum value*

As pointed out in the previous section, the drag is reduced owing to the increase in entrainment near the leading edge. There appear to be two important factors for the optimum drag reduction: there should be an increase in entrainment and it should occur close to separation. Consequently, the faster the shear layer can be made to grow, the smaller the drag will be. The growth rate will depend on how well the excitation is amplified and where the amplification occurs.

In trying to understand the mechanics of these effects, it was concluded that an important element of the flow structure is the final vortex of the shear layer before reattachment. The scales of this vortex are more closely tied to the overall dimensions

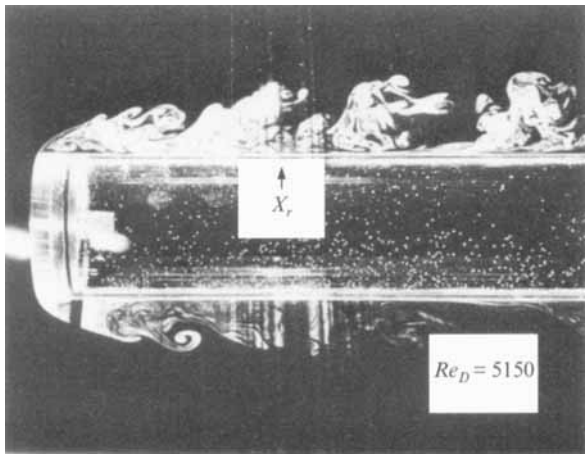

FIGURE 8. Laser-induced fluorescence visualization in water, unforced flow.

of the separation bubble than to those of the initially separating shear layer. In this it has similarities to the von Kármán cylinder shedding problem and the 'preferred mode' of the circular jet described in Crow & Champagne (1971). An important conclusion is that there are two fundamentally different instabilities involved: the Kelvin–Helmholtz instability of the free shear layer, and the 'shedding' type instability of the entire bubble. These are different, but not necessarily uncoupled. The basic difference is that the free shear layer vorticity interacts with itself, while the 'shedding' instability results from interaction of the vorticity with the wall. (From here on, this instability will be referred to as the 'shedding' instability. It will only be defined in terms of the analogy with von Kármán vortex shedding. More details of its nature will be discussed in §4.5.) This is an interaction with vorticity of the opposite sign, the image vorticity resulting from the presence of the wall. It is hypothesized that the greatest drag reduction results from forcing at frequencies which are amplified by both the Kelvin–Helmholtz and the shedding instability. Figure 6(*b*) shows structures that are clearly interacting with the wall, and the value of $F_{ex} D/U_\infty = 1.64$ is near the optimum range of 2 to 3.

This two-instability approach to the problem was prompted by some observations made in the unforced bubble (although it is well established in the case of cylinder shedding and the 'preferred mode' of the circular jet). Figure 8 is a laser-induced fluorescence photograph of the unforced flow in a water channel with a $Re_D = 5150$. Dye was introduced far upstream ahead of the contraction, so that probe interference was minimized. The cylinder was made of Plexiglas to allow the laser sheet to pass through it and cause the dye to fluoresce where the sheet and dye intersect. The dye impinging on the face of the cylinder acted as a tracer for the vorticity being generated there. Although its motion accounts primarily for the convective redistribution of vorticity and not the viscous diffusion (due to the high Schmidt number of water), locations of high dye concentration are indications of high vorticity concentration.

The striking conclusion from figure 8 is that there is a large quasi-periodic structure emerging from the bubble. This is the 'terminating' vortex which results from earlier amalgamations that cease when the vortex has grown to a size where its interaction with the wall becomes dominant and the flow reattaches. The terminating vortex of the shear layer at reattachment convects downstream. The final vortex of the shear layer becomes the first structure in the attached turbulent boundary layer. Further

amalgamations of this boundary layer structure may occur downstream, but at a much slower rate than in the preceding shear layer.

Large-scale vortices shed downstream of the separation bubble have been reported for the blunt flat plate, the two-dimensional analogue of the geometry discussed here (Hiller & Cherry 1981; Cherry *et al.* 1983, 1984; Kiya & Sasaki 1983*b*). It is expected that the cylinder flow is not qualitatively different, as the separation bubble height is only 20% of the diameter, and 7% of the circumference. This has been confirmed experimentally here. An unsteady three-dimensional structure for the reattaching zone and boundary layer has been proposed by Sigurdson & Roshko (1984), Kiya & Sasaki (1985), Sigurdson (1986), and Sasaki & Kiya (1991).

4.3. *Regimes of forcing* $F_{ex}D/U_\infty$

The concept of two different instabilities suggests four regimes for $F_{ex}D/U_\infty$ important to bubble forcing. These are, in order of descending frequency:

I $\quad F_{KH_i} \ll F_{ex}$;

II $\quad F_{shed} \ll F_{ex} \lesssim F_{KH_i}$;

III $\quad F_{shed} \approx F_{ex}$;

IV $\quad F_{ex} \ll F_{shed}$.

F_{shed} is the most amplified frequency of the shedding instability (discussed in detail in §4.5) and F_{KH_i} is the initial Kelvin–Helmholtz frequency (discussed in §4.4). Re_D is assumed to be high enough so that $F_{KH_i} \gg F_{shed}$.

Forcing in the first regime has little effect on C_{d_f} or X_r/D, as there is no instability to amplify the excitation. Shimizu *et al.* (1993) have found little effect for F_{ex} greater than twice F_{KH_i}. Forcing in the second regime is amplified by the shear layer. Oster & Wygnanski (1982) showed that the frequency of excitation determines the location downstream of separation where the perturbation can be amplified. The layer can amplify a broad band of frequencies around and lower than F_{KH_i} but limited by the available length before reattachment. In regime III, the shedding instability is primarily being driven and the maximum effect is observed. (In this instance $\approx$ means 'on the order of' F_{shed}). In regime IV, the shedding instability can no longer amplify the forcing, and there is little measured effect. For the values of Re_D discussed in these experiments, F_{KH_i} is always much greater than F_{shed}.

4.4. *Proposed scaling for* F_{KH_i}

Freymuth (1966) demonstrated that F_{KH_i} scales with convection velocity divided by the momentum thickness θ at separation:

$$F_{KH_i}\theta/U_c = \text{constant}. \tag{5}$$

Assuming that U_c scales with U_s and that the boundary layer on the cylinder face is laminar, the result is

$$\frac{F_{KH_i}D}{U_\infty} \propto \frac{U_s}{U_\infty} Re_D^{1/2}. \tag{6}$$

(Numerical estimates (Sigurdson 1986) indicate that the boundary layer on the face is stable up to $Re_D = 10^9$, greater than any Re_D discussed here. This is due to the strong favourable pressure gradient approaching the separation point.) Equation (6) accounts for the effect of the changing U_s on U_c, and changing Re_D on θ. It does not account for the effect on θ resulting from the altered velocity distribution on the cylinder face which would be expected to occur since U_s/U_∞ changes. With forcing, U_s increases and the velocity as a function of radius on the cylinder face is modified;

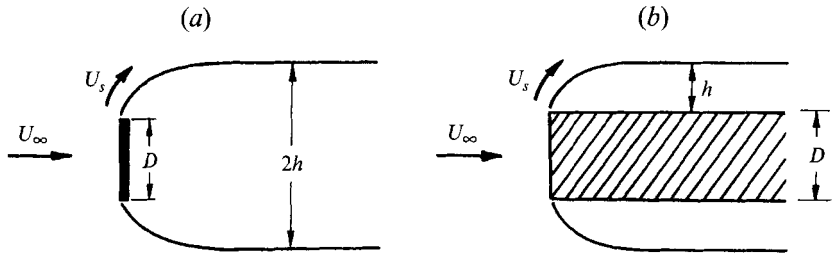

FIGURE 9. Schematic of the free-streamline technique: (*a*) the modified free streamline theory that was used; (*b*) choice of h for the present situation.

Geometry	$FD/U_\infty^\dagger$	$Fh/U_s^\dagger$	Reference
Free bubbles			
Circular cylinder	0.21	0.08	Roshko (1955)
90° wedge	0.18	0.08	Roshko (1955)
Bluff flat plate	0.14	0.08	Roshko (1955)
Wall-bounded bubbles			
Axisymmetric cylinder	0.4–0.5	0.07–0.09	Present result
	0.38, 0.48‡	0.07, 0.09‡	Kiya *et al.* (1991*a*)
Blunt flat plate	0.14	0.06	Cherry *et al.* (1983)
	0.12–0.13	0.07–0.08	Kiya *et al.* (1983*a*, 1985)
Backward-facing step	$Fh/U_\infty = 0.07$	0.07	Eaton & Johnston (1980)
Post-stalled airfoil		0.08	Zaman (1992)
Miscellaneous review	$FX_r/U_\infty = 0.5$–0.8	$Fh/U_\infty = 0.07$–0.11	Mabey (1972)
Forced wedge	$F_{ex}h/U_\infty = 0.075$	≈ 0.075	Koga *et al.* (1984)

† Unless otherwise noted.
‡ The first number is pressure fluctuations, the second is flow reversals.

TABLE 1. Non-dimensionalized 'shedding' frequencies

therefore, even if Re_D is unchanged, θ at separation will be altered. In order to take this into account an individual calculation of θ would need to be made, a simple scaling would not suffice. Equation (6) is not an unreasonable approximation however, and is included to show how F_{KH_i} increases with Re_D.

4.5. *Proposed scaling for* F_{shed}

The basic hypothesis behind the proposed scaling for F_{shed} (for the axisymmetric geometry as well as the blunt flat plate) is that the instability is *like* Kármán vortex shedding from a cylinder but the vortex interaction is with *image* vortices due to the wall rather than *actual* ones. The instability is slightly different from that which forms the Kármán vortex street in that this instability involves a symmetric street of vortices (as a result of the mirror nature of the image vortices) as opposed to the staggered asymmetric street arrangement which was shown to be stable by von Kármán & Rubach (1912). This similarity to Kármán vortex shedding suggests that a scaling similar to that used by Roshko (1955) for cylinders of differing cross-sectional shape may apply. Figure 9(*a*) shows a schematic of the modified free streamline theory that was used. The measured C_{p_s} was used to give U_s from (3), and the corresponding separating free streamline was calculated to give h, which for that case was the half-width of the wake. It was found that although $F_{shed}D/U_\infty$ has values of 0.21 for a circular cylinder, 0.18 for a 90° wedge, and 0.14 for a bluff plate, $F_{shed}h/U_s = St_h$ (Strouhal number based on h) had a universal value of 0.08 for all cases (table 1).

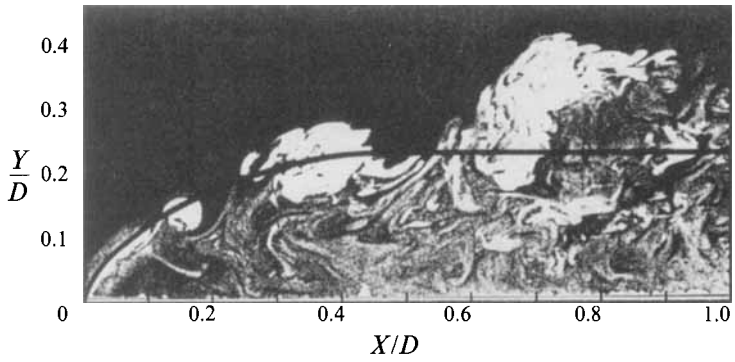

FIGURE 10. Superimposed free streamline, $Re_D = 16240$.

Figure 9(*b*) shows how h should be chosen for the present situation. In analogy to cylinder shedding, h represents the half distance between the vorticity and its corresponding image of opposite sign. The technique used to calculate the separating streamlines in figure 6 has been developed by using the two-dimensional hodograph theory developed by Roshko (1954) and the analysis reported in Koenig (1978) and Koenig & Roshko (1985) which relates the bubble height to C_{p_s} for an axisymmetric body. That analysis has been extended to accommodate blockage (Sigurdson 1986, 1995). It is based on equating the theoretical drag for the potential flow over a semi-infinite body in a channel (therefore accommodating blockage) with the estimated drag on the cylinder face and separating streamline based on the measured C_{p_s}. The latter is estimated from (1), C_{p_s} and the projected area (in the axial direction) of the free-stream surface. This analysis provides h/d, given C_{p_s}, through the following equation:

$$C_{p_s} = \frac{1}{1-1.25(1+2h/D)^2}\left(1+\frac{1.25\beta(1+2h/D)^4}{1-\beta(1+2h/D)^2}\right), \tag{7}$$

where $\beta = \pi D^2/4A$ and A is the wind tunnel cross-sectional area. Then the two-dimensional theory of Roshko (1954) can be used to provide a free streamline which has this h/D. Figure 10 is included as an indication of how well the theory predicts the free streamline shape when blockage is low ($Re_D = 16240$, the same model as figure 8).

The expected result is that

$$F_{shed}\, h/U_s = \text{constant}, \tag{8}$$

therefore

$$\frac{F_{shed}\, D}{U_\infty} \propto \frac{D}{h}\frac{U_s}{U_\infty}. \tag{9}$$

The non-dimensional shedding frequency is only an indirect function of Re_D through its effects on h/D and U_s/U_∞, effects which are relatively weak when compared to the direct $Re_D^{1/2}$ dependence of $F_{KH_i} D/U_\infty$ shown in (6).

4.6. *Results of the scaling*

There are two main uses for the proposed scaling. It allows some understanding of the effects of varying the frequency of excitation. It also correlates the 'shedding' frequency range which occurs for a variety of geometries and is discussed in the following sections.

For the structures in figure 8, $F_{shed}\, D/U_\infty$ can be estimated from their wavelength ($\lambda/D = 1.0$) assuming that $U_c = 0.5\, U_\infty$ (measured by Kiya & Sasaki 1983*b*). The result is $F_{shed}\, D/U_\infty = 0.5$ and with $h/D = 0.23$ and $U_s/U_\infty = 1.27$ (estimated from Ota's

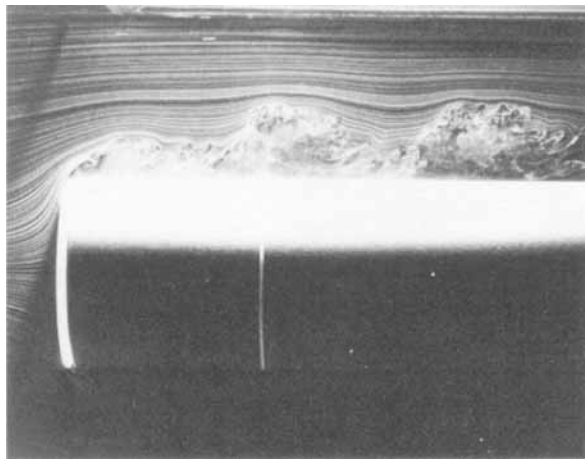

FIGURE 11. Forced case, $Re_D = 22000$, $F_{ex} D/U_\infty = 1.6$, $u'/U_\infty = 21\%$.

1975 result for C_{p_s} and (3)), the value of $F_{shed} h/U_\infty = 0.09$. Kiya *et al.* (1991*a*) for the unforced coaxial cylinder bubble found a peak at $FX_r/U_\infty = 0.6$ in the cylinder surface pressure spectrum measured near reattachment multiplied by the frequency (F), which they stated reflected the shedding of large-scale vortices. The frequency of shifting of flow direction at reattachment was $FX_r/U_\infty = 0.77$, which might also reflect the passage of vortices, but not necessarily only the large-scale ones. Kiya & Sasaki (1985) suggest that this type of difference may be caused by 'the dispersion of large scale vortices in strength and position'. The blockage was 1.7%, therefore h/D would be expected to be similar to that inferred here from Ota's (1975) measured C_{p_s}, $h/D = 0.23$. Kiya found $X_r/D = 1.60$ and $U_s/U_\infty = 1.27$ (Ota 1975); therefore we can estimate $Fh/U_s = 0.07$ in this case for the pressure and $Fh/U_s = 0.09$ for the shifting of flow direction.

All of these values are close to the value of 0.08 reported in Roshko (1955) for the Kármán vortex street. Other evidence indicating the universality of this scaling is provided through comparison with other flow geometries in §4.8 and table 1. Although it is not unexpected that this scaling should work, the fact that the numerical value is similar for wall-bounded flows and Kármán shedding is. Although they are both generically similar phenomena, Kármán vortex shedding is largely unsymmetrical whereas here symmetry is imposed by the reflection condition.

The plane wake behind a two-dimensional object can, however, have both the symmetrical (varicose) and antisymmetrical (sinuous) modes of instability. Wygnanski, Champagne & Marasli (1986) showed that the varicose mode cannot be neglected in considering the development of the wake over long distances, but rather an interaction between both modes must be considered. They point out that previously the parallel mean flow assumption led to the neglect of the varicose mode because of its smaller rate of amplification, and that the most unstable frequency of the varicose mode is only a bit higher than a subharmonic of the most unstable frequency of the sinuous mode. As the varicose mode is shown to be an important part of the wake instability, it is therefore not unreasonable to hypothesize that the present situation can represent this mode. The predicted frequency of the varicose mode being near a subharmonic of the sinuous mode would at first appear to be problematic and needs further consideration. That prediction is, however, based on a parallel flow hypothesis which is not true for the present case, and therefore linear stability analysis would not be expected to be accurate.

Experiment number	u' (m s^{-1})	U_∞ (m s^{-1})	u'/U_∞ (%)	Re_D
1	0.47	12.0	3.9	126600
2	0.47	8.0	5.9	84400
3	0.94	12.0	7.8	127300
4	0.94	8.0	11.8	84400
5	0.47	4.0	11.8	42200
6	0.94	4.0	23.6	42400

TABLE 2. Experimental conditions for acoustic forcing

Quantity	Magnitude
ΔC_{p_s}	−48%
ΔX_r	−58%
ΔU_s	13%
Δh	−48%
ΔC_{d_f}	−15%
ΔSt_h	−53%

TABLE 3. Maximum effects of forcing

For the forcing conditions shown in figure 6(*b*), the value of $F_{ex}h/U_s = 0.16$, twice the expected value of $F_{shed}h/U_s = 0.08$. The pairing implied by the photograph suggests that the resulting structure shed from the bubble has $F_{shed}h/U_\infty = 0.08$. This observation is reinforced by the photograph in figure 11, which has the same $F_{ex}D/U_\infty$ as figure 6(*b*), but with a higher amplitude of excitation, $u'/U_\infty = 21\%$. The distinct structures downstream of reattachment have a value of λ corresponding to half the value of F_{ex}.

4.7. *More experiments and discussion*

In total, six experiments are reported for various Re_D and u'/U_∞, broadening the range of forcing amplitudes examined. The experimental conditions are listed in table 2. Values of u'/U_∞ ranged from 3.9% to 23.6%. The maximum effects of the forcing are summarized in table 3.

Figure 12(*a*) plots drag reduction versus F_{ex}. It indicates that there is quite a varied response to the frequency of forcing and that there are no clear individual frequencies which characteristically bring a large effect at all the different flow velocities, which might be an indication of peculiarities in the forcing apparatus at that frequency. It also shows a quite different response to forcing for the two different flow velocities (and therefore Reynolds number) at the 11.8% level. Figure 12(*b*) plots drag reduction versus $F_{ex}D/U_\infty$, and shows a trend for the minimum in the drag to occur at higher values of $F_{ex}D/U_\infty$ and over a broader range for higher values of u'/U_∞. Note also that now the two curves for $u'/U_\infty = 11.8\%$ are quite similar despite the large Re_D difference. This indicates that Re_D, which affects F_{KH_i}, is not of primary importance at these high values of Re_D. The reason that the minimum swings from values of $F_{ex}D/U_\infty$ of 2.5 to 4 as forcing amplitude is increased is that the natural bubble 'shedding' frequency is getting higher owing to reduced h and increased U_s. In support of this conclusion and the hypothesized scaling, figure 12(*c*) shows how, on plotting versus $F_{ex}h/U_s$, the minima of the curves occur at the same value of $F_{ex}h/U_s$. The broadness of the range for maximum effect also becomes similar.

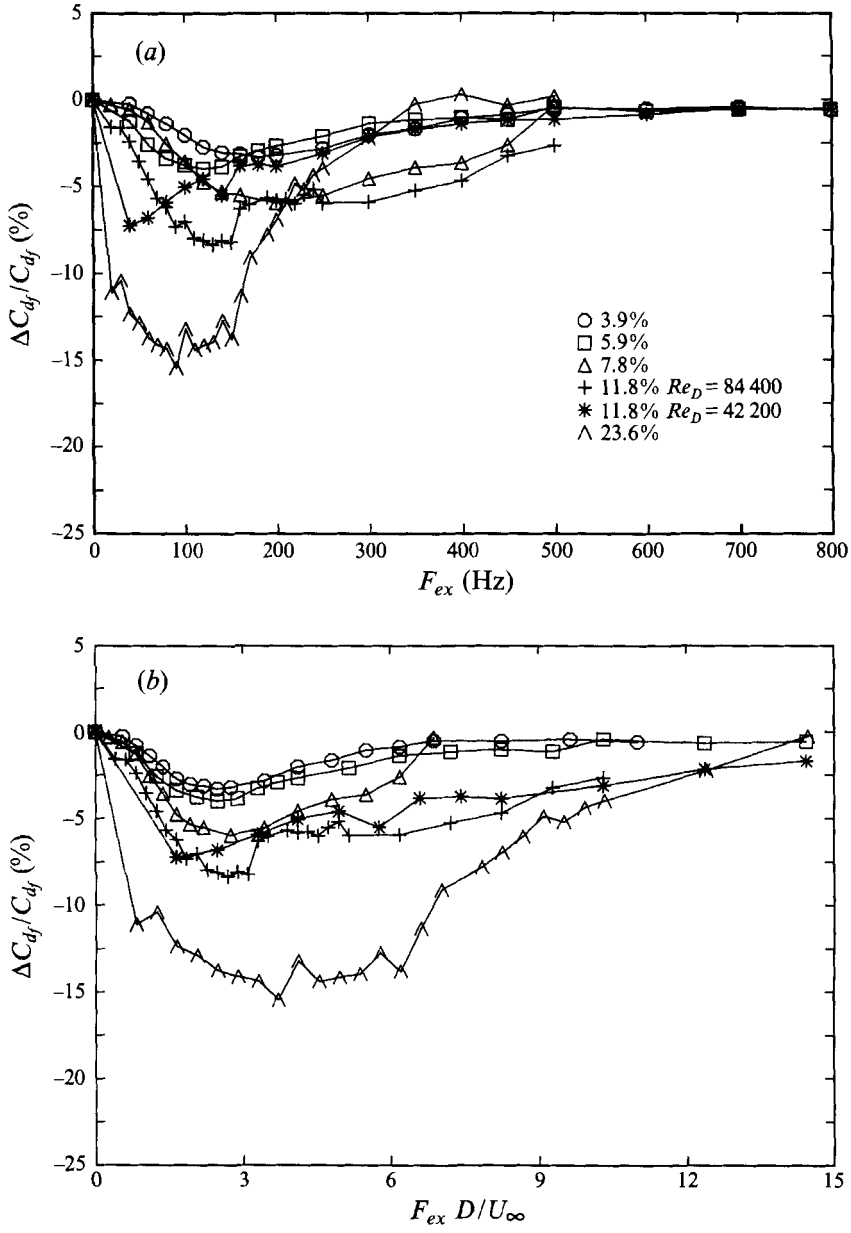

FIGURE 12 (*a*, *b*). For caption see facing page.

Figure 13 indicates that the maximum drag reduction possible at any u'/U_∞ is a linear function of u'/U_∞. The data can be reduced one more step by normalizing the drag reduction with the maximum possible drag reduction at that particular value of u'/U_∞. This result is plotted in figure 14. It can be seen that the minimum drag occurs for values of $F_{ex}h/U_s$ between approximately 0.16 and 0.40. The data collapse for values of $F_{ex}h/U_s$ near and less than that for maximum drag reduction (regime III and lower frequencies), indicating a linear response to the forcing. The shedding instability is primarily being forced in that regime. For greater values of $F_{ex}h/U_s$ (regime II), the curves do not collapse, indicating that the free shear layer response is much more

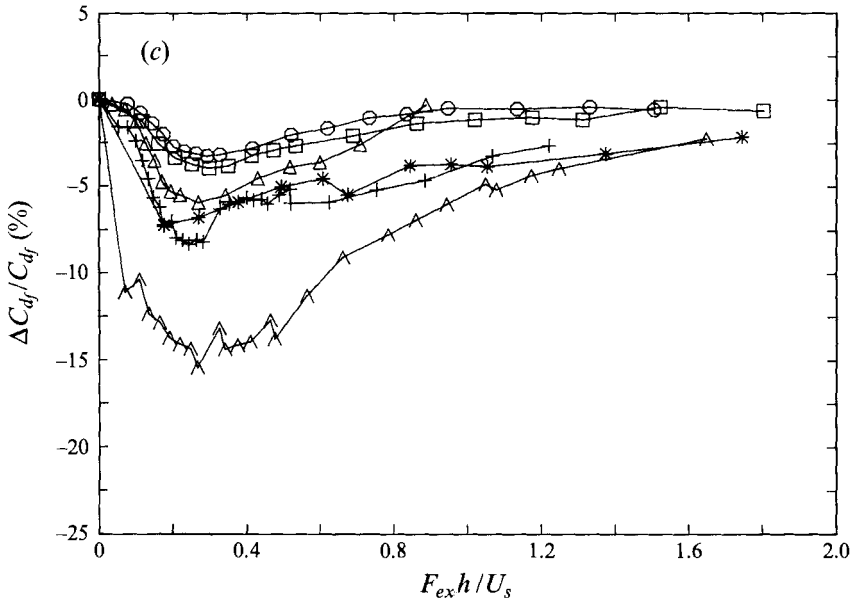

FIGURE 12. Drag reduction versus (*a*) F_{ex}, (*b*) $F_{ex}D/U_\infty$, (*c*) $F_{ex}h/U_s$.

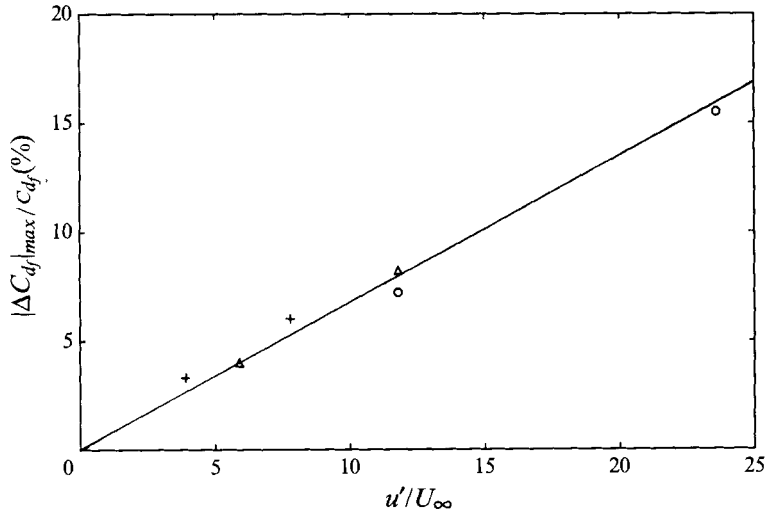

FIGURE 13. Maximum drag reduction versus u'/U_∞: ○, $Re_D = 42000$; △, 84000; +, 127000.

complex. This complex behaviour is expected, because the most-amplified frequency of the shear layer does not scale with h, but with the local shear layer thickness. The location of the increased entrainment resulting from forcing is important in the determination of C_{p_s} and therefore C_{d_f}. It is known (Oster & Wygnanski 1982) that the forcing amplifies at the downstream location where the shear layer has grown to the appropriate thickness. This location of amplification could be a function of forcing amplitude, since the separation bubble properties vary with forcing amplitude. For instance, at high amplitudes of forcing such as in figure 5, it is apparent that the amplification occurs immediately downstream of separation, independent of F_{ex}. This would not be expected at lower amplitudes.

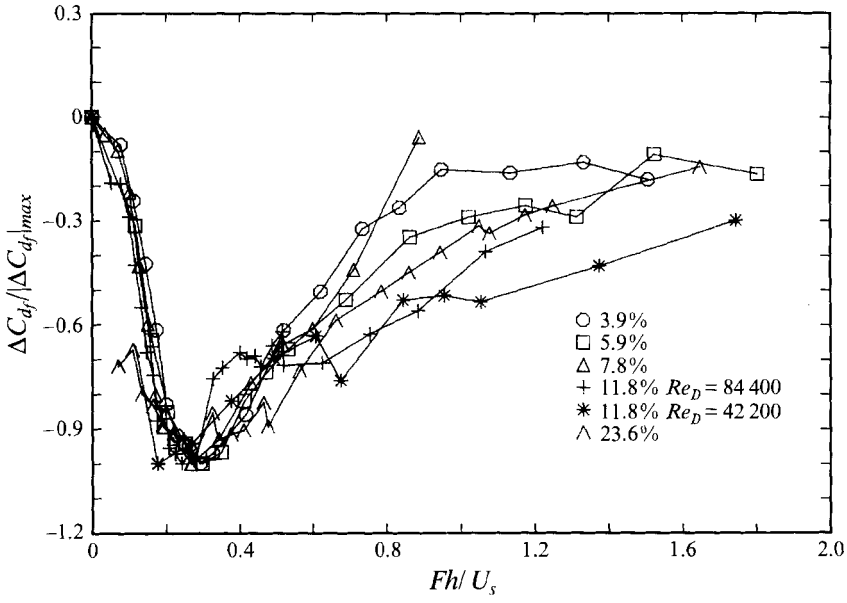

FIGURE 14. Normalized drag reduction versus Fh/U_s.

The results of figure 14 suggest that F_{ex} for minimum C_{d_f} is between two and five times higher than the most-amplified shedding frequency. The $F_{ex}D/U_\infty$ range of roughly 1–6 (depending on forcing amplitude) in figure 12(*b*) for minimum drag corresponds to $F_{ex}h/U_s = 0.16$ to 0.40. This is consistent with the hypothesized requirement for minimum drag that the entrainment be increased near the separation line, the nearer the better. It may also be a consequence of the diminution of the imposed excitation with distance from the leading edge, as is discussed in the apparatus section. This would result in better amplification at higher values of F_{ex} which could amplify closer to the origin of excitation, where the excitation is strongest.

The dependence of the most-amplified frequency on h/D and U_s/U_∞ has a complicating consequence. When exciting the bubble, both of these quantities change, so that it cannot be stated *a priori* what the optimum forcing frequency will be.

Equation (4) for λ_{ex}/D can be rewritten to give

$$\frac{\lambda_{ex}}{h} = \frac{1}{2}\left(\frac{F_{ex}h}{U_s}\right)^{-1}. \tag{10}$$

For the minimum drag range of $F_{ex}h/U_s$ of 0.16 to 0.40, this results in values of λ_{ex}/h from 3.1 to 1.3. Therefore, as noted earlier in the flow visualization results, the minimum drag corresponds to values of λ_{ex} comparable to the bubble height.

It might be expected that there is a certain amount of coupling between the shear layer and shedding instabilities for certain conditions. Then there would be evidence in the data, for example plateaus in the frequency response. Such evidence is not clearly present, although it may be manifested in more obscure ways, for instance the nonlinear response in regime II. Three possible reasons for this will be presented.

First, Re_D is quite high for these experiments and therefore there is a broad range of frequencies that are amplified, bounded by F_{KH_i} at the top end down to F_{shed} and possibly below. This means that for the experiments reported here, there may be between three and five pairings necessary before the initial Kelvin–Helmholtz vortices

have amalgamated into a final shedding vortex, there being a factor of 10 to 20 between F_{shed} and F_{KH_i}. All this pairing activity allows a very broad band of amplification which would not be expected to provide plateaus in the frequency response. At lower Re_D than those studied here, if F_{shed} and F_{KH_i} were near each other (for instance if F_{shed} were the subharmonic of F_{KH_i}) perhaps more distinct coupling behaviour would be observed.

Second, the initial Kelvin–Helmholtz frequency appears experimentally to be in a fairly broad band. Therefore it is not expected that there is a discrete subharmonic, but at least a similarly broad band.

Third, most of the data here are forced at frequencies less than F_{KH_i}, with the exception of experiments 5 and 6 in table 2. Experiments 1 to 4 have estimated values of F_{KH_i} ranging from 2600 to 1400 Hz, with forcing frequencies up to 500 and 800 Hz. Experiments 5 and 6 have a measured F_{KH_i} in a broad band around 500 Hz, with forcing frequencies up to 800 and 500 Hz, respectively. (The reason for the difference in maximum F_{ex} is that the higher levels of u' could not be sustained at the higher frequencies.)

For a very similar forcing geometry, Shimizu *et al.* (1993) focused their attention on the reattachment length X_r rather than C_{p_s} or C_{d_f}. In their figure 6, for values of F less than the optimum, monotonic behaviour appears with increasing forcing amplitude. For values greater than optimum, a more complicated behaviour appears, similar to the present data. A swing in their values of $F_{ex}D/U_\infty$ for maximum results can also be seen, similar to our figure 12(*b*): a swing from values of 1.5 to 2.4 for forcing levels between values of 0.5 and 10%. This compares to a swing from 2.5 to 2.6 for forcing levels of 3.9 to 11.8% in the present data. The shedding instability is no doubt a factor in explaining their results as well, but the frequency for maximum effect appears to be lower than in the present case.

For example, at 6% forcing they found $F_{ex}D/U_\infty \approx 1.8$ is best ($Re_D = 69000$) whereas it is 2.6 at 5.9% in the present case ($Re_D = 84400$). This difference is most likely due to the reduced $h/D = 0.20$ (versus 0.23 unblocked) and increased $U_s/U_\infty = 1.43$ (versus 1.27 unblocked) in the present case due to blockage. We can test the hypothesis by trying to account for this effect in the following way. We do not know h/D and U_s/U_∞ for Shimizu *et al.*'s (1993) forced bubble, but we can estimate it for the unforced bubble as we did earlier from Ota's (1975) results. If we do this, their $F_{ex}D/U_\infty = 1.8$ becomes $F_{ex}h/U_s = 0.33$. If we use the corresponding h/D and U_s/U_∞ for the unforced bubble in the present case, $F_{ex}D/U_\infty = 2.6$ becomes $F_{ex}h/U_s = 0.36$, a value quite close to Shimizu *et al.*'s (1993) 0.33. This suggests that the hypothesis is correct, and the same shedding instability is being forced in Shimizu *et al.*'s (1993) case. This approach of using the unforced h/D and U_s/U_∞ in the scaling is expected to hold in this case since the forcing levels are approximately the same, otherwise this would not be the case.

This kind of frequency rescaling can be done to all of the 6% forcing data from Shimizu *et al.* (1993) and 5.9% data from here. The question is: what would a suitable vertical axis be to allow a more complete comparison? One possibility would be to take the percentage reduction data for X_r and C_{d_f} and normalize it with its maximum reduction. This is plotted in figure 15. The agreement is remarkably good, considering that estimates were used for h and U_s. This is strong evidence for the validity of the proposed scaling for the shedding instability and the validity of both sets of experimental data. It also reinforces the idea that the criteria for minimum drag are the same as for minimum reattachment length.

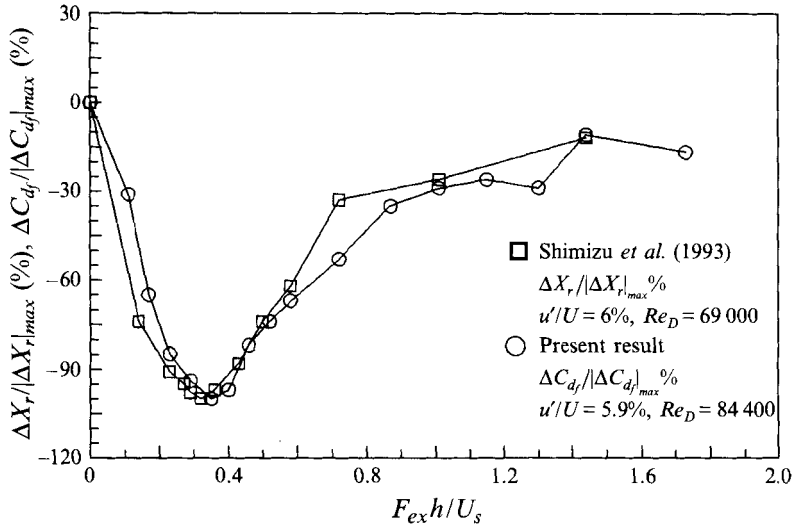

FIGURE 15. Percentage reduction in X_r (Shimizu *et al.* 1993) and C_{d_f} normalized with maximum reduction.

4.8. *Comparison with other geometries*

The proposed scaling appears to also apply to separation bubbles occurring in other geometries, both unforced and forced. The non-dimensionalized frequencies for a variety of bubbles are summarized in table 1.

For the blunt flat plate, Cherry *et al.* (1983, 1984) obtained a value of $FD/U_\infty = 0.14$ for pressure fluctuations at reattachment (in the following paragraphs F is a frequency measured in the flow using various methods), which corresponds to $Fh/U_s = 0.06$ (using their measured value of C_{p_s}, which gives $U_s/U_\infty = 1.3$ and thus $h/D = 0.51$ from the two-dimensional hodograph theory). Kiya & Sasaki (1983*a*) for the same geometry found $FD/U_\infty = 0.12$ from the cross-spectra and coherence of surface pressure and velocity fluctuations. Using their measured value of $h/D = 0.7$ (obtained from their dividing streamline) and U_s/U_∞ of approximately 1.25 gives a value of $Fh/U_s = 0.07$. (They found that $h/X_r \approx 0.14$, therefore $X_r \approx 7h$ is a typical value which will be used later for estimates for other bubble results. Perhaps because Cherry *et al.* (1983) suggested it and X_r is easier to measure than h, they use it as the relevant length scale.)

Sutton *et al.* (1981) excited the separation bubble at the sharp-edged inlet to a pipe using a vibrating surface near the separation edge. They found that the reattachment length could be reduced by more than one third when forcing at $F_{ex}D/U_s = 1.8$ (where D is the pipe diameter). An approximate value of $h/D = 0.2$ can be estimated from their data, which results in a value of $F_{ex}h/U_s = 0.36$. This is within the frequency range of 0.16 and 0.40 found here for optimum results. They also found a lack of response for values of $F_{ex}h/U_s$ less than 0.1 which is well below the bottom end of the optimum range.

For the backward-facing step Eaton & Johnston (1980) found a spectral peak near reattachment with $Fh/U_\infty = 0.07$. This needs no renormalization to be consistent with the present scheme, since $U_\infty = U_s$ for the step and h is equal to step height. Also for the backward-facing step, Bhattacharjee *et al.* (1986) found in acoustic forcing experiments that the separated mean flow spreading rate could be increased most

effectively by forcing at $F_{ex}h/U_s$ (where h is step height) between 0.2 and 0.4. This corresponds well with the optimum forcing frequency of between 0.16 and 0.40 in the present experiment.

Nishioka, Asai & Yoshida (1990) used incident acoustic excitation to control the leading-edge flow separation on an airfoil. They referred to Sigurdson & Roshko (1988) and noted that their flow responded in a similar fashion to frequencies lower than the 'naturally occurring waves due to the inflectional instability' and that the effective frequency scales with the height of the separation bubble. They supported the idea of Sigurdson & Roshko (1988) that the phenomenon is similar to Kármán vortex shedding, although they added that the details of the nonlinear instability needed to be clarified.

Zaman (1992) studied the effect of acoustic excitation on post-stalled flows over airfoils, where the flow is fully separated from near the leading edge. Under the influence of excitation a tendency toward reattachment occurred (although the flow might still be fully separated), lift was increased and drag reduced. When the amplitude of forcing was increased it was found that the optimum effect occurred at progressively lower values of frequency, contrary to the present case. The reason for this may have been that a source of sound external to the wing was used which may have forced the higher-frequency shear layer Kelvin–Helmholtz instability at low amplitudes and the lower-frequency shedding instability at higher amplitudes.

Zaman referenced Sigurdson & Roshko (1985) and reviewed his results taking into account the concept that $F_{ex}h/U_s$ was the relevant non-dimensionalization. The value of h and U_s could be estimated from velocity profile measurements and a value of approximately 0.08 was obtained for the effective frequency. Zaman noted that this was 'interestingly close to the so-called shedding instability frequency' and concluded that the idea of the instability and its importance to the excitation of separated flows over wings deserved further investigation.

Brocher (1977), reporting on a Euromech Colloquium, noted that Lebouché & Martin described the flow in a duct which has a sudden enlargement on both sides, a rearward-facing step. A critical reduced frequency of free-stream pulsation of $Fh/U_s \approx 0.07$ was found. For values of reduced frequency less than this, the recirculation vortex was shed. For greater values, the vortex was stable but smaller than for steady flow. Interpretation of these results is limited as the Reynolds number was not reported; however, it is interesting to note the value of 0.07 appearing.

Mabey (1972) reported that the spectra of pressure fluctuations near the reattachment line are similar if non-dimensionalized with the bubble length for bubbles caused by leading-edge separation on wings, forward-facing steps, rearward-facing steps, sudden enlargements in pipes, and cavities. Peak pressure fluctuations occurred for values of FX_r/U_∞ between 0.5 and 0.8. A typical value of X_r/h is 7, which results in values of Fh/U_∞ between 0.07 and 0.11. The broadness of this range and its mean might be reduced if U_s were used in the normalized frequency rather than U_∞.

In studying the effect of an oscillating flap on the reattaching flow behind a two-dimensional wedge, Koga *et al.* (1984) found that the most effective reattachment control occurred near values of $F_{ex}h/U_\infty$ of about 0.075. They also noted that 'control' could be achieved by the generation of vortices with sizes that are on the order of the separation height, supporting the conclusion of Sigurdson *et al.* (1981).

Levi (1983) proposed a universal 'Strouhal law' for the relationship between the frequency of oscillation, U_∞, and a typical width (d) of the 'fluid body', for a wide variety of fluid phenomena. These included wakes, jets, shock waves, cavitation, wing auto-rotation, vortex breakdowns, and surface and internal waves. The value

of $Fd/U_\infty = 0.16$ was claimed for all cases, which would correspond to a value of $Fh/U_\infty = 0.08$, since d would be $= 2h$.

5. Conclusions

An apparatus has been designed and constructed to study the effect of excitation on a reattaching flow. The flow is considerably modified when forced at frequencies for which associated wavelengths are comparable to the separation bubble height. At the high Reynolds numbers investigated here, these wavelengths are greater than and the forcing frequencies are lower than those of the initial Kelvin–Helmholtz frequencies of the separating free shear layer. Forcing then increases entrainment in the early part of the shear layer; as a result, reattachment length, bubble height, pressure at separation, and drag on the face are all reduced. Table 3 summarizes the maximum change for each of these quantities. Larger effects were observed under less controlled circumstances.

In the unforced flow there is a natural 'shedding' frequency, analogous to that in wakes of bluff bodies and to the 'preferred mode' frequency in the early axisymmetric jet. There are two fundamentally different instabilities involved: the Kelvin–Helmholtz instability of the free shear layer and the 'shedding'-type instability of the entire bubble which is controlled by interaction with the wall.

The method of frequency scaling proposed ($F_{shed}\,h/U_s$), based on an analogy with cylinder vortex shedding, correlates frequency data for separation bubbles occurring in a variety of geometries which reattach on walls. This scaling results in values of $F_{shed}\,h/U_s$ near 0.08, the value for cylinder shedding. This is surprising because, although they are generically similar phenomena, Kármán vortex shedding is unsymmetrical whereas separation bubbles that reattach on walls have symmetry imposed by the reflection condition.

Four regimes of forcing have been proposed. In the first, the forcing frequency is much greater than the initial Kelvin–Helmholtz frequency and any frequency the shear layer can amplify. In the second, the shear layer amplifies the forcing, but the drag reduction results for a specified non-dimensional forcing frequency are not linear with forcing amplitude. In the third regime, the shedding instability is being forced and the drag reduction is linear with forcing amplitude for a fixed non-dimensional frequency. Forcing in the fourth regime at frequencies much less than the shedding frequency has little measured effect. The initial Kelvin–Helmholtz frequencies seemed irrelevant to the results reported here. At lower Reynolds numbers this is not expected to be so.

The maximum drag reduction behaves linearly with forcing amplitude. The minimum drag (regime III) occurs over a $F_{ex}\,D/U_\infty$ range of roughly 1 to 6, and a range of 0.16 to 0.40 in $F_{ex}\,h/U_s$, between two and five times the expected value of 0.08 for the most amplified shedding frequency. This suggests that the minimum occurs when the initial shear layer is used to amplify the forcing, creating structures that amalgamate to form a final structure with $F_{shed}\,h/U_s = 0.08$. A comparison of optimum frequencies of excitation with measurements made by other researchers is quite favourable. The three-dimensional nature of the shedding instability discussed in Sigurdson & Roshko (1984) and Sigurdson (1986) may explain why the F_{ex} must be greater than the first harmonic of F_{shed}, since each shed structure is thought to often consist of a pairing of the final two shear layer structures before reattachment. The role of the shear layer instability and its interaction with the shedding instability requires further study.

The dependence of the most amplified shedding frequency on h/D and U_s/U_∞ makes it difficult to predict what the optimum forcing frequency will be. The use of free

streamline theory simplifies this problem by relating these quantities to the measured value of the pressure coefficient at separation.

Most of this work was done at the Aeronautics Department, California Institute of Technology. It is based on work for a PhD thesis (Sigurdson 1986) and thanks are given for the help of my advisor, Dr Anatol Roshko, who's influence is evident throughout. Mr Bill Peck and anonymous reviewers are thanked for their assistance. Financial support for this research was provided by the Office of Naval Research, contract number N00014-76-C-0260.

REFERENCES

AHUJA, K. K., WHIPKEY, R. R. & JONES, G. S. 1983 Control of turbulent boundary layer flows by sound. *AIAA Paper* 83-0726.

BAR-SEVER, A. 1989 Separation control on an airfoil by periodic forcing. *AIAA J.* **27**, 820–821.

BHATTACHARJEE, S., SCHEELKE, B. & TROUTT, T. R. 1986 Modification of vortex interactions in reattaching separated flow. *AIAA J.* **24**, 623–629.

BROCHER, E. 1977 Oscillating flows in ducts: a report on Euromech 73. *J. Fluid Mech.* **79**, 113–126.

BROWN, G. L. & ROSHKO, A. 1974 On density effects and large structure in turbulent mixing layers. *J. Fluid Mech.* **64**, 775–816.

CHERRY, N. J., HILLIER, R. & LATOUR, M. 1983 The unsteady structure of two-dimensional separated and reattaching flows. *J. Wind Engng Indust. Aerodyn.* **11**, 95–105.

CHERRY, N. J., HILLIER, R. & LATOUR, M. E. M. P. 1984 Unsteady measurements in a separated and reattaching flow. *J. Flow Mech.* **144**, 13–46.

COLLINS, F. G. 1981 Boundary-layer control on wings using sound and leading edge serrations. *AIAA J.* **19**, 129–130.

COLLINS, F. G. & ZELENEVITZ, J. 1975 Influence of sound upon separated flow over wings. *AIAA J.* **13**, 408–410.

CORKE, T., KOGA, D., DRUBKA, R. & NAGIB, H. 1977 A new technique for introducing controlled sheets of streaklines in wind tunnels. *IEEE Publication* 77-CH 1251-8 AES.

CROW, S. C. & CHAMPAGNE, F. H. 1971 Orderly structure in jet turbulence. *J. Fluid Mech.* **48**, 151–159.

EATON, J. K. & JOHNSTON, J. P. 1980 Turbulent flow reattachment: an experimental study of the flow and structure behind a backward-facing step. *Thermosciences Div., Dept. of Mech. Engng, Stanford, Rep.* MD-39.

EATON, J. K. & JOHNSTON, J. P. 1981 A review of research on subsonic turbulent flow reattachment. *AIAA J.* **19**, 1093–1100.

FREYMUTH, P. 1966 On transition in a separated laminar boundary layer. *J. Fluid Mech.* **25**, part 4, 683–704.

GAD-EL-HAK, M. 1990 Control of low-speed airfoil aerodynamics. *AIAA J.* **28**, 1537–1552.

GAD-EL-HAK, M. & BUSHNELL, D. M. 1991 Separation control: review. *Trans ASME* I: *J. Fluids Engng* **113**, 5–30.

HILLER, R. & CHERRY, N. J. 1981 The effects of stream turbulence on separation bubbles. *J. Wind Engng Indust. Aerodyn.* **8**, 49–58.

HSIAO, F. B., LIU, C. F. & SHYU, J. Y. 1990 Control of wall-separated flow by internal acoustic excitation. *AIAA J.* **28**, 1440–1446.

HUANG, L. S., MAESTRELLO, L. & BRYANT, T. D. 1987 Separation control over an airfoil at high angles of attack by sound emanating from the surface. *AIAA Paper* 87-1261.

KÁRMÁN, T. VON & RUBACH, H. 1912 Über den mechanismus des flüssigkeits – und luftwiderstandes. *Physik. Z.* **13**, 49–59.

KELSO, R. M., LIM, T. T. & PERRY, A. E. 1993 The effect of forcing on the time-averaged structure of the flow past a surface-mounted bluff plate. *J. Wind Engng Indust. Aerodyn.* **49**, 217–226.

KIYA, M., MOCHIZUKI, O., IDO, Y. & KOSAKU, H. 1993*a* Structure of turbulent leading-edge separation of a blunt circular cylinder and its response to sinusoidal disturbances. *J. Wind Engng Indust. Aerodyn.* **49**, 227–236.

KIYA, M., MOCHIZUKI, O., IDO, Y. & KOSAKU, H. 1993*b* Effects of periodic forcing on a turbulent separation zone of a blunt circular cylinder. *Trans. JSME* B **59**, 366–373 (in Japanese).

KIYA, M., MOCHIZUKI, O., TAMURA, H., NOZAWA, T., ISHIKAWA, R. & KUSHIOKA, K. 1991*a* Turbulence properties of an axisymmetric separation-and-reattaching flow. *AIAA J.* **29**, 936–941.

KIYA, M., MOCHIZUKI, O., TANAKA, H. & TSUKASAKI, T. 1991*b* Control of a turbulent leading-edge separation bubble. In *Separated Flows and Jets* (ed. V. V. Kozlov & A. V. Dovgal), pp. 647–656. Springer.

KIYA, M. & SASAKI, K. 1983*a* Free-stream turbulence effects on a separation bubble. *J. Wind Engng Indust. Aerodyn.* **14**, 375–386.

KIYA, M. & SASAKI, K. 1983*b* Structure of a turbulent separation bubble. *J. Fluid Mech.* **137**, 83–113.

KIYA, M. & SASAKI, K. 1985 Structure of large-scale vortices and unsteady reverse flow in the reattaching zone of a turbulent separation bubble. *J. Fluid Mech.* **154**, 463–491.

KIYA, M., SASAKI, K. & ARIE, M. 1982 Discrete-vortex simulation of a turbulent separation bubble. *J. Fluid Mech.* **120**, 219–244.

KOENIG, K. 1978 Interference effects on the drag of bluff bodies in tandem. PhD thesis, Calif. Inst. Technology.

KOENIG, K. & ROSHKO, A. 1985 An experimental study of geometrical effects on the drag and flow field of two bluff bodies separated by a gap. *J. Fluid Mech.* **156**, 167–204.

KOGA, D. J., REISENTHEL, P. & NAGIB, H. M. 1984 Control of separated flowfields using forced unsteadiness. *Illinois Inst. Technology Fluids and Heat Transfer Rep.* R84-1.

LANE, J. C. & LOEHRKE, R. I. 1991 Leading edge separation from a blunt plate at low Reynolds number. *Trans. ASME* I: *J. Fluids Engng* **102**, 494–496.

LEVI, E. 1983 A universal Strouhal law. *ASCE J. Engng Mech.* **109**, 718–727.

MABEY, D. G. 1972 Analysis and correlation of data on pressure fluctuations in separated flow. *J. Aircraft* **9**, 642–645.

MIAU, J. J., LEE, K. C., CHENG, M. H. & CHOU, J. H. 1991 Control of separated flow by a two-dimensional oscillating fence. *AIAA J.* **29**, 1140–1148.

MONTIVIDAS, R. E., ACHARYA, M. & METWALLY, M. H. 1992 Reactive control of an unsteady separating flow. *AIAA J.* **30**, 1133–1134.

NISHIOKA, M., ASAI, M. & YOSHIDA, S. 1990 Control of flow separation by acoustic excitation. *AIAA J.* **28**, 1909–1915.

OSTER, D. & WYGNANSKI, I. 1982 The forced mixing layer between parallel streams. *J. Fluid Mech.* **123**, 91–130.

OTA, T. 1975 An axisymmetric separated and reattached flow on a longitudinal blunt circular cylinder. *Trans. ASME* E: *J. App. Mech.* June 311–315.

OTA, T. & MOTEGI, H. 1980 Turbulence measurements in an axisymmetric separated and reattached flow over a longitudinal blunt circular cylinder. *Trans. ASME* E: *J. App. Mech.* **47**, 1–6.

PARKER, R. & WELSH, M. C. 1983 Effects of sound on flow separation from blunt flat plates. *Intl J. Heat Fluid Flow* **4**, 113–127.

ROBERTS, F. A. 1985 Effects of a periodic disturbance on structure and mixing in turbulent shear layers and wakes. PhD thesis, Aeronautics Dept., Calif. Inst. Technology.

ROOS, F. W. & KEGELMAN, J. T. 1986 Control of coherent structures in reattaching laminar and turbulent shear layers. *AIAA J.* **24**, 1956–1963.

ROSHKO, A. 1954 A new hodograph for free streamline theory. *NACA Tech. Note* 3168.

ROSHKO, A. 1955 One the wake and drag of bluff bodies. *J. Aero. Sci.* **22**, 1, 124–132.

SASAKI, K. & KIYA, M. 1991 Three-dimensional vortex structure in a leading-edge separation bubble at moderate Reynolds numbers. *Trans. ASME* I: *J. Fluids Engng* **113**, 405–410.

SHIMIZU, M., KIYA, M., MOCHIZUKI, O. & IDO, Y. 1993 Response of an axisymmetric separation bubble to sinusoidal forcing. *Trans. JSME* B **59**, 721–727 (in Japanese).

SIGURDSON, L. W. 1986 The structure and control of a turbulent reattaching flow. PhD Thesis, Aeronautics Dept., Calif. Inst. Technology.

SIGURDSON, L. W. 1995 Techniques for approximating and transition of separation bubbles on blunt-faced cylinders aligned coaxially with the free-stream. *AIAA J.* (submitted).

SIGURDSON, L. W., CIMBALA, J. & ROSHKO, A. 1981 Controlled excitation of a separated flow. *Bull. Am. Phys. Soc.* **26**, 1275.

SIGURDSON, L. W. & ROSHKO, A. 1984 The large-scale structure of a turbulent reattaching flow. *Bull. Am. Phys. Soc.* **29**, 1542.

SIGURDSON, L. W. & ROSHKO, A. R. 1985 Controlled unsteady excitation of a reattaching flow. *AIAA Paper* 85-0552.

SIGURDSON, L. W. & ROSHKO, A. 1988 The structure and control of a turbulent reattaching flow. In *Turbulence Management and Relaminarisation* (ed. H. W. Liepmann & R. Narasimha), pp. 497–514. Springer.

SORIA, J., SHERIDAN, M. & WU, J. 1993 Spatial evolution of the separated shear layer from a square leading-edge flat plate. *J. Wind Engng Indust. Aerodyn.* **49**, 237–246.

SUTTON, E. P., EVANS, G. P., MCGUINESS, M. D. & SVEHLA, K. M. 1981 Influence of wall vibrations on a flow with boundary-layer separation at a convex edge. In *Unsteady Turbulent Shear Flows* (ed. R. Michel, J. Cousteix & R. Houdeville), pp. 285–293. Springer.

VIETS, H. 1979 Coherent structures in time dependent shear flows. In *Proc. NATO AGARD Conf. 271 on Turbulent Boundary Layers, Experiments, Theory and Modelling*, pp. 5.1–5.14. The Hague, The Netherlands.

VIETS, H. & PIATT, M. 1981 Induced unsteady flow in a dump combustor. In *Combustion in Reactive Systems* (ed. J. R. Bowen, A. K. Oppenheim & R. I. Soloukhin), *Progress in Astronautics and Aeronautics*, vol. 76, pp. 611–624.

WELSH, M. C. & GIBSON, D. C. 1979 Interaction of induced sound with flow past a square leading edged plate in a duct. *J. Sound Vib.* **67**, 501–511.

WINANT, C. D. & BROWAND, F. K. 1974 Vortex pairing: the mechanism of turbulent mixing layer growth at moderate Reynolds number. *J. Fluid Mech.* **63**, 237–255.

WYGNANSKI, I., CHAMPAGNE, F. & MARASLI, B. 1986 On the large-scale structures in two-dimensional, small-deficit, turbulent wakes. *J. Fluid Mech.* **168**, 31–71.

ZAMAN, K. B. M. Q. 1992 Effect of acoustic excitation on stalled flows over an airfoil. *AIAA J.* **30**, 1492–1499.

ZAMAN, K. B. M. Q., BAR-SEVER, A. & MANGALAM, S. M. 1987 Effect of acoustic excitation on the flow over a low-Re airfoil. *J. Fluid Mech.* **182**, 127–148.